Calculation of the polarization of light emitted during electron-impact excitation of Ba^+

Christopher J. Bostock,* Dmitry V. Fursa, and Igor Bray
ARC Centre for Antimatter-Matter Studies, Curtin University, GPO Box U1987, Perth, Western Australia 6845, Australia
(Received 31 March 2014; revised manuscript received 30 May 2014; published 13 June 2014)

The measurements of Crandall *et al.* [Phys. Rev. A **10**, 141 (1974)] for the polarization of light emitted during electron-impact excitation of Ba^+ are in significant disagreement with relativistic distorted wave scattering theory calculations of Sharma *et al.* [Phys. Rev. A **83**, 062701 (2011)]. The relativistic convergent close-coupling (RCCC) method is applied to the problem and the discrepancy between theory and experiment is resolved across the full range of energies measured. Furthermore, the oscillations in the polarization fraction measurements at low energies near threshold are reproduced by the RCCC calculations and linked to the formation of autoionizing states of neutral Ba.

DOI: 10.1103/PhysRevA.89.062710 PACS number(s): 34.80.Dp

I. INTRODUCTION

The polarization of light emitted during electron-impact excitation of ions provides a diagnostic tool for plasmas [1] and in addition provides a sensitive testing ground for scattering theories [2]. In this latter context, the measurements of Crandall *et al.* [3], made four decades ago, for the polarization of light emitted in the electron-impact excitation of the $(6s)\ ^2S_{1/2} \rightarrow (6p)\ ^2P_{3/2}$ transition in Ba^+ have yet to be reproduced by any scattering theory. The results of existing relativistic distorted wave scattering calculations [4] are in serious disagreement with the measurements. It was claimed in [4] that cascade contributions from higher states could be the source of the discrepancy. This provides the motivation to revisit the problem utilizing the relativistic convergent close-coupling (RCCC) formalism which is suitable for the calculation of spin-dependent and polarization observables of quasi-one- and two-electron targets [5–11].

Previously the RCCC method has been applied to resolve a long-standing discrepancy for the polarization of x rays emitted by highly charged ions during electron-impact excitation [12]. In that case, the Breit interaction, a relativistic correction to the Coulomb potential, was responsible for bringing theory into alignment with experiment. In the present case of electron scattering from Ba^+, the measurements of Crandall *et al.* [3] were performed at relatively low energies (2–750 eV) where Breit interaction effects are negligible. Application of the RCCC method to the calculation of the polarization fraction has yielded excellent agreement with the original measurements. Cascade contributions were also calculated, but found to have only a minor contribution.

II. METHOD

The Ba^+ ion is modeled as one active valence electron above an inert Xe Dirac-Fock core. The Xe Dirac-Fock core orbitals are obtained using the GRASP package [13]. For the Ba^+ valence electron, a set of one-electron orbitals is obtained by diagonalization of the quasi-one-electron Dirac-Coulomb Hamiltonian in a relativistic (Sturmian) L-spinor basis [14]. Phenomenological one- and two-electron polarization potentials are used to improve the accuracy of the calculated Ba^+ wave functions [15,16]; these allow us to take into account more accurately the effect of closed inert shells on the active electrons. The one-electron polarization potential parameters depend on the static dipole polarizability of the inert Ba^{2+} core which was chosen as $\alpha_c = 14.5$. The parameters of the polarization potentials, the fall-off radius $r_c^{\rm pol}$ and $r_c^{\rm diel}$, are adjusted to obtain the best representation of target state energies and optical oscillator strengths. For the Ba^{2+} core we chose an l-dependent $r_c^{\rm pol}$ with values 3.1, 3.2, 3.13, and 2.27 for $l = 0,1,2,3$, respectively. For the two-electron polarization potential we chose $\alpha_c = 10.61$ [17] and $r_c^{\rm diel} = 3.5$. Our target model consists of 51 states—35 bound states and 16 continuum states. The energy levels of the first ten states used in the calculations are listed in Table I, and the effective oscillator strengths for the $(6s)\ ^2S_{1/2} \rightarrow (6p)\ ^2P_{1/2}$ and $(6s)\ ^2S_{1/2} \rightarrow (6p)\ ^2P_{3/2}$ resonance transitions are listed in Table II. The oscillator strength for the $(6s)\ ^2S_{1/2} \rightarrow (6p)\ ^2P_{3/2}$ transition is slightly higher than experiment which is an indication of the imperfection in the Xe inert core model.

The target states are then used to expand the total wave function of the electron-Ba^+ scattering system and formulate a set of relativistic Lippmann-Schwinger equations for the T-matrix elements. In this latter step, the relativistic Lippmann-Schwinger equations for the T-matrix elements have the following partial wave form:

$$T_{fi}^{\Pi J}(k_f\kappa_f,k_i\kappa_i) = V_{fi}^{\Pi J}(k_f\kappa_f,k_i\kappa_i) + \sum_n \sum_\kappa \int\!\!\!\!\!\!\diagup\!\!\!\!\!\!\int dk \frac{V_{fn}^{\Pi J}(k_f\kappa_f,k\kappa) T_{ni}^{\Pi J}(k\kappa,k_i\kappa_i)}{E - \epsilon_n^N - \epsilon_{k'} + i0}. \quad (1)$$

The notation in Eq. (1), the matrix elements, and the method of solution using a hybrid OpenMP-MPI parallelization suitable for high performance supercomputing architectures is given in Ref. [19].

The polarization of light emitted from the $(6p)\ ^2P_{3/2}$ state depends on the magnetic sublevel populations [20,21],

$$P = \frac{3(\sigma_{1/2} - \sigma_{3/2})}{3\sigma_{3/2} + 5\sigma_{1/2}}, \quad (2)$$

where σ_{m_f} is the cross section for excitation to a magnetic sublevel of the $(6p)\ ^2P_{3/2}$ state.

*c.bostock@curtin.edu.au

TABLE I. Energy levels of the first ten Ba^+ states calculated by diagonalizing the target in the RCCC method. Experiment levels listed by NIST [18] are also shown.

Configuration	RCCC (eV)	Experiment (eV)
$(6s)\ ^2S_{1/2}$	0.000	0.000
$(5d)\ ^2D_{3/2}$	0.610	0.604
$(5d)\ ^2D_{5/2}$	0.672	0.704
$(6p)\ ^2P_{1/2}$	2.518	2.512
$(6p)\ ^2P_{3/2}$	2.725	2.722
$(7s)\ ^2S_{1/2}$	5.278	5.251
$(6d)\ ^2D_{3/2}$	5.736	5.697
$(6d)\ ^2D_{5/2}$	5.758	5.722
$(4f)\ ^2F_{5/2}$	6.002	5.983
$(4f)\ ^2F_{7/2}$	6.003	6.011
Ionization limit	10.007	10.000

Cascades from the high-lying excited levels to the $(6p)\ ^2P_{3/2}$ state can affect the polarization of the $(6p)\ ^2P_{3/2} \rightarrow (6s)\ ^2S_{1/2}$ line. We take into account the cascades by using the method described in Ref. [12]. The contribution to the $(6p)\ ^2P_{3/2}$ state magnetic sublevel cross section σ_{m_f} from an upper-lying state n with cross section σ_{m_n} is

$$\sigma_{m_f}^{\mathrm{casc},m_n} = \sigma_{m_n} b(n,f) \langle j_f m_f 1q | j_n m_n \rangle^2, \tag{3}$$

where $\langle j_f m_f 1q | j_n m_n \rangle$ is a Clebsch-Gordan coefficient and $b(n,f)$ is the branching ratio for dipole radiative decay from the upper level n to the lower level f. By applying this formula to all possible radiative decay paths and summing over all bound states we obtain an estimate of the total cascade correction

$$\sigma_{m_f}^{\mathrm{app}} = \sigma_{m_f} + \sum_n \sum_{m_n} \sigma_{m_f}^{\mathrm{casc},m_n}. \tag{4}$$

The cascade corrected magnetic sublevels can then be used to calculate the polarization fraction via Eq. (2).

III. RESULTS

In Fig. 1 we present RCCC results for the polarization of light emitted in the $(6p)\ ^2P_{3/2} \rightarrow (6s)\ ^2S_{1/2}$ transition due to electron-impact excitation of Ba^+. A comparison is made with the measurements of Crandall *et al.* [3] and the relativistic distorted wave scattering calculations of Sharma *et al.* [4] (labeled RDW in the figure). In general, there is excellent agreement between the RCCC results and the measurements, and the discrepancy between experiment and previous RDW calculations is resolved. RCCC results with cascade contributions are also shown, and it is apparent that

TABLE II. Oscillator strengths of the Ba^+ ground state compared to experimental values listed by NIST [18].

	Oscillator strength	
Transition	RCCC	Expt.
$(6s)\ ^2S_{1/2} \rightarrow (6p)\ ^2P_{1/2}$	0.349	0.348
$(6s)\ ^2S_{1/2} \rightarrow (6p)\ ^2P_{3/2}$	0.753	0.690

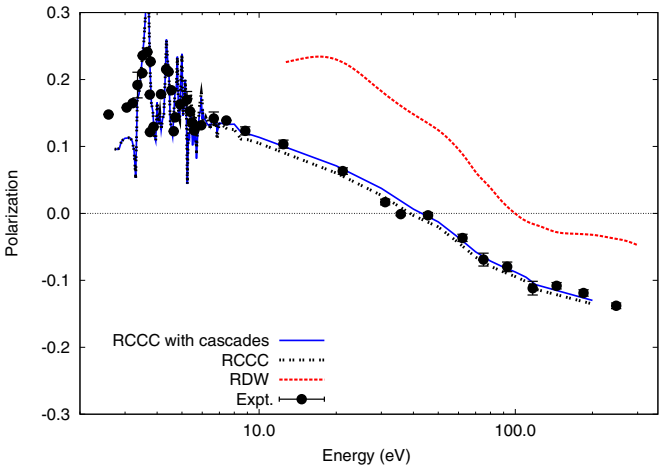

FIG. 1. (Color online) RCCC polarization fraction with and without cascades for excitation of the $(6s)\ ^2S_{1/2} \rightarrow (6p)\ ^2P_{3/2}$ transition in Ba^+. Measurements are due to Crandall *et al.* [3]; bars represent one standard deviation. The RDW results of Sharma *et al.* [4] are also shown. The polarization fraction is dimensionless.

cascades have a negligible effect on the polarization fraction. At high energies, particularly above 30 eV, corresponding to ten times the excitation threshold, it is surprising that the RDW results are not in agreement. In Table III we provide specific magnetic sublevel $\sigma_{m=1/2}$ and $\sigma_{m=3/2}$ cross sections at selected energies for the $(6p)\ ^2P_{3/2} \rightarrow (6s)\ ^2S_{1/2}$ transition. The polarization fraction is determined by substituting the magnetic sublevel cross sections into Eq. (2). By performing a series of convergence studies (not presented) we estimate that the presented results are converged to within 1%.

The low-energy (3–6 eV) RCCC results (with cascade contributions included) are examined on a finer energy mesh in Fig. 2. At energies just above the $(6s)\ ^2S_{1/2} \rightarrow (6p)\ ^2P_{3/2}$ excitation threshold the effects of close coupling are most evident. The polarization measurements exhibit significant oscillations in this region and the RCCC results generally reproduce these oscillations except for distinct peaks that are not observed in the measurements. This is likely to be due to the finite resolution of the electron beam. Crandall *et al.* [3] state that "the natural maxima and minima may be much higher and lower than shown." This is indeed evident in Fig. 2 where the RCCC results map the shape of the oscillations in the measurements with the additional features of extra sharp maxima and minima in the RCCC results.

The structures in the polarization function are an indication of strong projectile-target electron correlations. As discussed

TABLE III. Magnetic sublevel $\sigma_{m=1/2}$ and $\sigma_{m=3/2}$ cross sections for the $(6s)\ ^2S_{1/2} \rightarrow (6p)\ ^2P_{3/2}$ transition at selected energies. Cross sections for the direct transition (denoted "dir") are compared with the cascade corrected cross sections (denoted "cas").

Energy (eV)	$\sigma_{1/2\ \mathrm{dir}}$	$\sigma_{1/2\ \mathrm{cas}}$	$\sigma_{3/2\ \mathrm{dir}}$	$\sigma_{3/2\ \mathrm{cas}}$
10.0	18.8	23.0	14.0	16.8
20.0	14.6	17.6	12.4	14.5
50.0	9.0	10.4	9.5	10.8

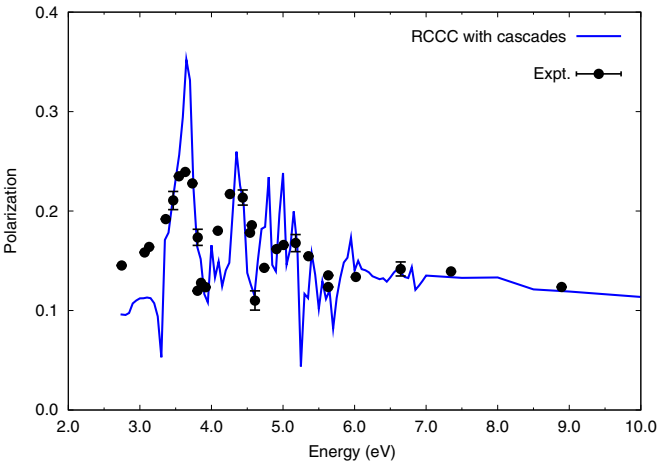

FIG. 2. (Color online) RCCC polarization fraction for excitation of the $(6s)\ ^2S_{1/2} \rightarrow (6p)\ ^2P_{3/2}$ transition in Ba^+. Measurements are due to Crandall *et al.* [3]; bars represent one standard deviation. The polarization fraction is dimensionless.

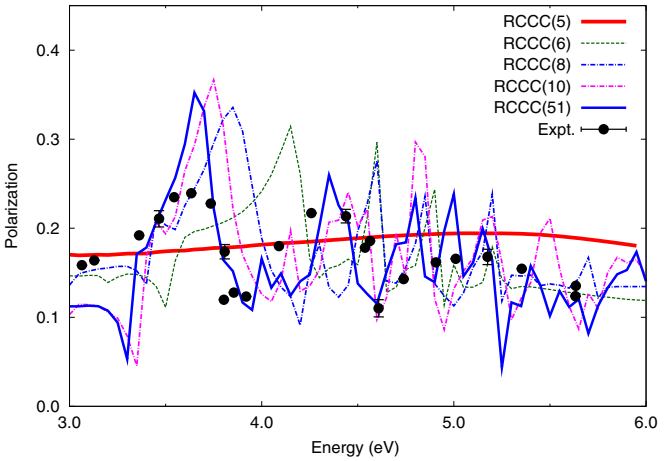

FIG. 3. (Color online) RCCC polarization fraction for excitation of the $(6s)\ ^2S_{1/2} \rightarrow (6p)\ ^2P_{3/2}$ transition in Ba^+. The states used in each calculation are given in Table IV. Measurements are due to Crandall *et al.* [3]; bars represent one standard deviation. The polarization fraction is dimensionless.

by Fano and Macek [22] if such correlations are of sufficient duration (in excess of 10^{-14} s) a substantial exchange of angular momentum can occur between the electrons. This can lead to a corresponding reduction of the polarization of the emitted radiation. The formation of autoionizing states of the neutral barium atom as a reaction channel in electron scattering from Ba^+ ion is the most obvious source of such strong correlations. Crandall *et al.* [3] suggested that these autoionizing levels should have configurations $7snl$ and $6dnl$.

In order to identify possible autoionizing states of Ba that are responsible for the structures in the polarization fraction curve we have conducted a sequence of progressively larger RCCC calculations as specified in Table IV with results presented in Fig. 3. The RCCC(5) calculation uses only the first five states: $(6s)\ ^2S_{1/2}$, $(5d)\ ^2D_{3/2}$, $(5d)\ ^2D_{5/2}$, $(6p)\ ^2P_{1/2}$, and $(6p)\ ^2P_{3/2}$. This model does not account for any autoionizing states above the highest energy state of Ba^+ included in the calculation—the $(6p)\ ^2P_{3/2}$ state in the RCCC(5) model. In the region from 3 to 6 eV, where the experiment shows strong resonance behavior, this model does not have any autoionizing states and we should expect a smooth polarization fraction curve. This is indeed the case as can be seen from Fig. 3.

The RCCC(6) calculation includes an extra state $(7s)\ ^2S_{1/2}$. This allows us to account for the neutral Ba autoionizing states with $7snl$ configurations that are located below the threshold of the Ba^+ $(7s)\ ^2S_{1/2}$ state. Figure 3 demonstrates that the RCCC(6) model does have a strong resonance behavior though the positions of the resonance structures are very different when compared with the experiment and the converged RCCC(51) results. The addition of $(6d)\ ^2D_{3/2}$ and $(6d)\ ^2D_{5/2}$ states in the close-coupling expansion, the RCCC(8) model, allows us to include the autoionizing states with $6dnl$ configurations. It is evident that the RCCC(8) model produces results that begin to map the structures in the polarization fraction. Similarly, in the RCCC(10) model, which also includes the $(4f)\ ^2F_{5/2}$ and $(4f)\ ^2F_{7/2}$ states in the close-coupling expansion, the structures become even more pronounced and closer to the converged results.

This analysis indicates that a large number of reaction channels leading to various autoionizing states as well as the channel coupling between all reaction channels are responsible for the formation of resonance structures in the polarization fraction.

TABLE IV. States used in different RCCC calculations.

Calculation	States employed
RCCC(5)	$(6s)\ ^2S_{1/2}$,$(5d)\ ^2D_{3/2}$,$(5d)\ ^2D_{5/2}$,$(6p)\ ^2P_{1/2}$,$(6p)\ ^2P_{3/2}$
RCCC(6)	RCCC(5) + $(7s)\ ^2S_{1/2}$
RCCC(8)	RCCC(6) + $(6d)\ ^2D_{3/2}$ + $(6d)\ ^2D_{5/2}$
RCCC(10)	RCCC(8) + $(4f)\ ^2F_{5/2}$ + $(4f)\ ^2F_{7/2}$

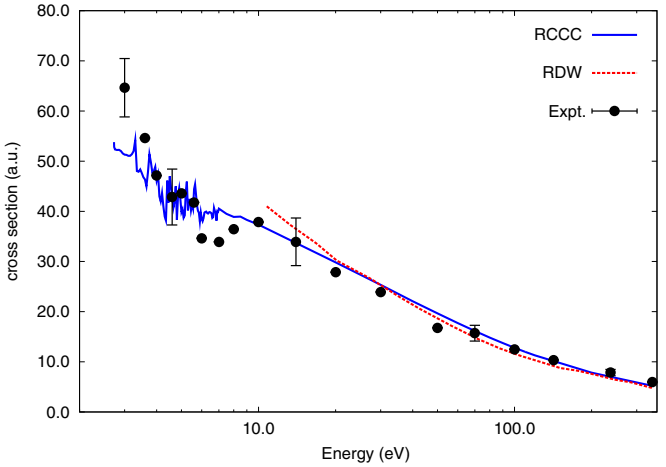

FIG. 4. (Color online) RCCC integrated cross section for the $(6s)\ ^2S_{1/2} \rightarrow (6p)\ ^2P_{1/2}$ transition in Ba^+. Measurements are due to Crandall *et al.* [3] with cascade contributions subtracted; bars represent uncertainties. The RDW results of Sharma *et al.* [4] are also shown. The integrated cross sections are given in atomic units (a.u.).

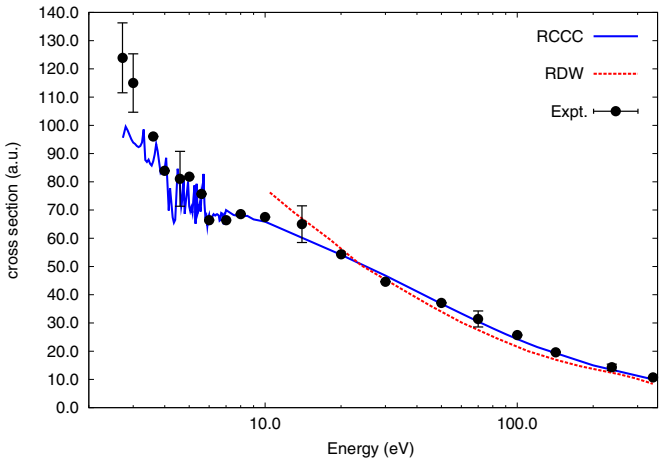

FIG. 5. (Color online) RCCC integrated cross section for the $(6s)\ ^2S_{1/2} \rightarrow (6p)\ ^2P_{3/2}$ transition in Ba^+. Measurements are due to Crandall *et al.* [3] with cascade contributions subtracted; bars represent uncertainties. The RDW results of Sharma *et al.* [4] are also shown. The integrated cross sections are given in atomic units (a.u.).

Figures 4 and 5 show the RCCC integrated cross section results for the $(6s)\ ^2S_{1/2} \rightarrow (6p)\ ^2P_{1/2}$ and $(6s)\ ^2S_{1/2} \rightarrow (6p)\ ^2P_{3/2}$ transitions, respectively. Crandall *et al.* [3] provided direct cross sections with cascade contributions subtracted and therefore the RCCC results without cascades are presented. At high energies the RCCC results are in excellent agreement with experiment and the RDW results of Sharma *et al.* [4]. At low energies, below the region of validity of RDW calculations, the RCCC results are in reasonable agreement with experiment; a discrepancy exists for the $(6s)\ ^2S_{1/2} \rightarrow (6p)\ ^2P_{1/2}$ transition in the vicinity of 3 and 8 eV, and a similar discrepancy exists for the $(6s)\ ^2S_{1/2} \rightarrow (6p)\ ^2P_{1/2}$ transition in the region of 3 eV.

IV. CONCLUSION

We have resolved the discrepancy between theory [4] and experiment [3] in favor of experiment for the polarization of light emitted during the electron-impact excitation of the $(6s)\ ^2S_{1/2} \rightarrow (6p)\ ^2P_{3/2}$ transition in Ba^+. Cascade contributions to the polarization fraction are negligible. At low energies the RCCC results are able to reproduce the oscillations in the polarization fraction that are linked to the formation of autoionizing states of neutral Ba anticipated in the work of Crandall *et al.* [3]. At high energies, particularly above 30 eV (i.e., greater than ten times the excitation threshold), it is surprising that the relativistic distorted wave method of Sharma *et al.* [4] was unable to obtain the correct polarization fraction since we checked that our first-order results were not too different from the RCCC results presented on this energy range. For the integrated cross sections associated with excitation of the $(6p)\ ^2P_{1/2}$ and $(6p)\ ^2P_{3/2}$ states we find very good agreement with experiment, except for minor variations at low energies.

ACKNOWLEDGMENTS

The support of the Australian Research Council and Curtin University is acknowledged. We are grateful for access to the Australian National Computational Infrastructure and its Western Australian node iVEC.

[1] *Plasma Polarization Spectroscopy*, edited by T. Fujimoto and A. Iwamae, Springer Series on Atomic, Optical, and Plasma Physics (Springer, New York, 2007).
[2] N. Andersen and K. Bartschat, *Polarization, Alignment, and Orientation in Atomic Collisions* (Springer, New York, 2000).
[3] D. H. Crandall, P. O. Taylor, and G. H. Dunn, Phys. Rev. A **10**, 141 (1974).
[4] L. Sharma, A. Surzhykov, R. Srivastava, and S. Fritzsche, Phys. Rev. A **83**, 062701 (2011).
[5] D. V. Fursa and I. Bray, Phys. Rev. Lett. **100**, 113201 (2008).
[6] C. J. Bostock, D. V. Fursa, and I. Bray, Phys. Rev. A **89**, 032712 (2014).
[7] C. J. Bostock, D. V. Fursa, and I. Bray, Phys. Rev. A **88**, 062707 (2013).
[8] C. J. Bostock, D. V. Fursa, and I. Bray, J. Phys. B **45**, 181001 (2012).
[9] C. J. Bostock, D. V. Fursa, and I. Bray, Phys. Rev. A **85**, 062707 (2012).
[10] M. J. Berrington, C. J. Bostock, D. V. Fursa, I. Bray, R. P. McEachran, and A. D. Stauffer, Phys. Rev. A **85**, 042708 (2012).
[11] C. J. Bostock, M. J. Berrington, D. V. Fursa, and I. Bray, Phys. Rev. Lett. **107**, 093202 (2011).
[12] C. J. Bostock, D. V. Fursa, and I. Bray, Phys. Rev. A **80**, 052708 (2009).
[13] K. G. Dyall, I. P. Grant, C. T. Johnson, F. P. Parpia, and E. P. Plummer, Comput. Phys. Commun. **55**, 425 (1989).
[14] I. P. Grant and H. M. Quiney, Phys. Rev. A **62**, 022508 (2000).
[15] D. V. Fursa and I. Bray, J. Phys. B **30**, 5895 (1997).
[16] D. V. Fursa, I. Bray, and G. Lister, J. Phys. B **36**, 4255 (2003).
[17] S. H. Patil, At. Data Nucl. Data Tables **71**, 41 (1999).
[18] See http://physics.nist.gov/PhysRefData/ASD/levels_form.html.
[19] C. J. Bostock, J. Phys. B **44**, 083001 (2011).
[20] E. G. Berezhko and N. M. Kabachnik, J. Phys. B **10**, 2467 (1977).
[21] K. J. Reed and M. H. Chen, Phys. Rev. A **48**, 3644 (1993).
[22] U. Fano and J. H. Macek, Rev. Mod. Phys. **45**, 553 (1973).